Directed Assembly of Single Colloidal Gold Nanowires by AFM Nanoxerography

Pierre Moutet, Lise-Marie Lacroix, Antoine Robert, Marianne Imperor-Clerc, G. Viau, Laurence Ressier

Directed assembly of single colloidal gold nanowires by AFM nanoxerography

*Pierre Moutet,[a] Lise-Marie Lacroix,[a]*Antoine Robert,[a] Marianne Impéror-Clerc,[b] Guillaume Viau [a] and Laurence Ressier.[a]**

a. Université de Toulouse, LPCNO (Laboratoire de Physique et Chimie des Nano-Objets), UMR 5215 INSA-CNRS-UPS, 135 Avenue de Rangueil, F-31077 Toulouse, France

lmlacroi@insa-toulouse.fr; phone +33561559652, fax +33561559697

laurence.ressier@insa-toulouse.fr; phone +33561559672, fax +33561559697

b. Laboratoire de Physique de Solides, UMR 8502, Bat. 510, Université Paris-Sud, F-91405 Orsay, France

KEYWORDS. Metallic nanowires, directed assembly, AFM nanoxerography, electrostatic forces, ammonium chloride

ABSTRACT.

Ultrathin gold nanowires (NWs) dispersed in hexane were prepared by chemical reduction of $HAuCl_4$ in oleylamine, along with nanospheres (NSs), side products of the reaction. X-ray photoelectron spectroscopy and small angle X-ray scattering evidenced a stabilization of these nano-objects by oleylammonium chloride surfactants. The directed assembly of these nano-objects on surfaces was performed by atomic force microscopy (AFM) nanoxerography in a few seconds. Selective assembly of gold NWs only occured onto positively charged patterns while NSs assembled more specifically on the negatively charged ones. This sorting suggests that the strong electric field generated by the charge patterns induced a strong negative effective charge on the gold NWs and a weak positive effective charge on the NSs. Such difference could be explained by the ion organization at the colloid surface, monolayered in the case of NWs and bi-layered in the case of NSs. By adjusting the design of the positive patterns and the experimental conditions of development, single gold nanowires were successfully assembled by AFM nanoxerography on pre-defined sites of surfaces without damaging them, opening the way for future electrical and mechanical characterizations.

1. Introduction

The chemical synthesis in mild conditions of anisotropic colloidal nano-objects such as nanorods or nanowires led to highly crystalline nano-objects exhibiting enhanced physical properties such as high magnetic remanence.[1,2] Recently, colloidal gold (Au) nanowires (NWs) were obtained by reduction of a gold chloride precursor in presence of a long chain amine.[3] With their diameter below 2 nm, these ultrathin Au NWs represent fascinating systems likely to display electronic transport phenomena inerrant to the quasi one-dimensional confinement arising at the nanoscale.[4,5] However, such electronic transport studies require the addressing of individual NWs. In this aim, highly challenging technological steps must be overcome namely on i) the deposition and localisation of individual NWs on pre-defined areas of surface and ii) their electrical addressing. If their micrometric length opens the way to electrical connections by classical microelectronic processes,[6] their ultra-small diameters confer them an extreme fragility. Under external stress, they tend to break into spherical particles due to Rayleigh instability.[7] Regarding the first step of deposition and localisation, studies have mainly focused on the deposition of NWs by drop casting,[8] liquid-air interphase evaporation,[9] Langmuir-Blodgett,[10] or microfluidic techniques. [11] Based on these approaches, the conduction properties of Au NW bundles, were recently reported.[12,13,14,15,16] However, the experimental demonstration of clear correlations between the high aspect ratio of the nanowires and their conduction properties still requires measurements on individual nanowires.

Different approaches, such as dip-pen lithography,[17] convective self-assembly,[18] dielectrophoresis,[19] or nano-manipulation by atomic force microscopy (AFM)[20] have yet been used in the literature to assemble single colloidal nanoparticles on surfaces. However, these techniques suffer from at least one of the following disadvantages: high complexity, lack of

versatility, time consumption or restrictions on the size and geometry of the colloidal nano-objects. There is still a compelling need to develop a quick and versatile alternative to achieve directed assembly of any kind of single colloidal nano-objects, in particular anisotropic ones. Over the last past years, AFM nanoxerography has emerged as a highly versatile way to perform directed assembly of charged and/or polarizable colloidal nanoparticles dispersed into various polar or apolar solvents on surfaces.[21,22,23,24,25,26] It relies on selective electrostatic trapping of nano-objects onto charge patterns written by AFM on electret surfaces. A wide variety of nanoparticle assemblies such as binary, 3D or single nanoparticle assemblies with a fine control on the placement and organization of the nanoparticles have been achieved.[25,27] Except one isolated work on carbon nanotubes,[28] AFM nanoxerography has been used to perform directed assembly of spherical colloidal nanoparticles with sizes ranging from a few to hundreds of nanometers.

In this work, the capability of AFM nanoxerography for directed assembly of gold colloidal nanowires of a few micrometers length, dispersed in hexane, an apolar solvent, onto pre-defined areas of surfaces was investigated. By using charge patterns of opposite polarities, the ion organization at the surface of the two types of nano-objects present in solution, the gold nanowires of interest and the spheres, side products of the chemical reaction, was evaluated. On the basis of these results, the directed assembly ofsingle gold nanowires by AFM nanoxerography, was intended by adjusting the design and surface potential of the charge patterns.

2. Experimental section

2.1 Synthesis of gold nanowires

Ultrathin gold nanowires were prepared following a chemical synthesis adapted from B. Xing and co-workers,[3] as previously reported.[29] All reactants were used as received, oleylamine (OY, Aldrich, 70%) was stored under Ar blanket, triisopropylsilane (TIPS, Sigma Aldrich, 99%) and gold precursor (hydrogen tetrachloroaurate(III) trihydrate, $HAuCl_4 \cdot 3H_2O$, Alfa Aesar, 99,99%) were stored in a desiccator. Typically 10 mM solution of gold was prepared: 10 mg of $HAuCl_4 \cdot 3H_2O$ were dissolved in a solution containing 340 µL OY (400 mM, OY/Au = 40) in 1.65 mL of hexane (Alfa Aesar, >98%). 510 µL of TIPS, (1M, TIPS/Au = 100) were added to initiate the gold reduction. The solution was then kept undisturbed at 40°C for 3h30. The excess of ligands was removed by a classical precipitation process. 5 mL of absolute ethanol (Sigma Aldrich, > 99.8%) was added, the solution was centrifuged 5 min at 4000 rpm. The isolated colloids were redispersed in 1.5 mL of hexane to obtain a purified suspension with a mass concentration [Au] = 3 $g.L^{-1}$.

2.2 Characterization of the gold colloids

The colloids synthetized were characterized by transmission electron microscopy (TEM), using a 120 kV JEOL-1400 microscope. 100 µL of the purified suspension was diluted into 900 µL of hexane. Few drops of this dilution were deposited on carbon coated Cu grids.

X-ray photoelectron spectroscopy (XPS) spectra were recorded using a Kratos Analytical Limited Axis ultra-limited system fitted with a microfocused monochromatic Al Kα X-ray

source (1486.6 eV, 12kV , 120W). The pass energy was set at 160 eV and 20 eV for the survey and the regions spectra respectively.

Small Angle X-Ray Scattering (SAXS) measurements were performed on glass sealed capillaries (1.5 mm in diameter) containing the Au nanowire suspension as prepared and after purification. The experiments were performed using a monochromatic X-ray beam generated by a rotating anode X-ray source (Cu Kα, 50 kV, 50 mA). The instrument covers a range of scattering vectors q between 0.01 and 0.18 $Å^{-1}$. SAXS intensity was recorded on a CCD bi-dimensional detector placed inside a vacuum tube to reduce noise. For background subtraction, the capillary was measured first filled with pure solvent (hexane) before introducing the colloidal suspension (inside the same capillary).

2.3 AFM nanoxerography

Figure 1 presents the two step-protocol of AFM nanoxerography used to assemble gold NWs on surfaces. The first step consisted in writing charge patterns onto a 100 nm film of polymethylmethacrylate (PMMA), spin-coated on silicon wafers by applying 1ms voltage pulses at 50 Hz to a conductive AFM tip (Figure 1a). Two types of charge patterns were chosen in this study. The first type was used for evaluating the ion organization at the surface of NWs and studying their kinetics of assembly from the colloidal suspension onto the charge patterns. It consisted in two 3 µm squares of opposite polarities. Each square was made of multiple charge dots written using +80 V pulses for the positively charged one and -65 V for the negatively charged one, in order to ensure equivalent charging of each pattern.[30] The tip velocity was adjusted at 10 $µm.s^{-1}$, leading to 200 nm spacing between each charged dot. The second type of charge patterns, used to achieve a fine control of the directed assembly of single gold NWs,

consisted in 10 µm positively charged dotted lines. Spacing between dots ranged from 50 nm to 400 nm, by adjustment of tip velocity from 2.5 $\mu m.s^{-1}$ to 20 $\mu m.s^{-1}$. The voltage pulses were tuned between +30 V and +75 V.

For both types of charge patterns, the AFM z-feedback was adjusted to control the tip-sample distance during charge writing. Surface potential mapping of charge patterns was carried out by the AFM-based electric technique of amplitude modulation Kelvin Force Microscopy (KFM), using a lift height of 20 nm and a scan rate of 0.5 Hz.

The second step of the nanoxerography process consisted in developing the electrostatically patterned substrates into the colloidal suspension (Figure 1b). First, the purified colloidal suspension ([Au] = $3g.L^{-1}$) was sonicated 2 minutes and diluted 50 times leading to a gold concentration of 60 $mg.L^{-1}$. This suspension was then sonicated 30 seconds and diluted 25 times for the square patterns ([Au] = 2.4 $mg.L^{-1}$) or 100 times for the line patterns ([Au] = 0.6 $mg.L^{-1}$) respectively. Immersion of charge patterns into the colloidal suspension lasted from 5 to 30 seconds, followed by a 30 second rinsing in pure hexane. The samples were allowed to completely dry under ambient condition (P_{atm}, room temperature). Finally, NWs assemblies on charge patterns were characterized by topographical observations by AFM in tapping mode.

3. Results and Discussion

3.1. Characterization of the gold colloids

The reduction of $HAuCl_4$ by triisopropylsilane in presence of oleylamine led after only few hours to ultrathin Au nanowires and nanospheres as evidenced in Figure 2a. Diameters of 1.7 nm were deduced from TEM images and SAXS measurements for both, the spheres and the wires.[29] We

previously reported a detailed SAXS study on Au nanowires growth in their mother liquor, revealing the presence of a bilayer of surfactants at the surface of the wires.[29] The same study also revealed a volume fraction of 5.3×10^{-5} and 1.8×10^{-5} for the wires and the spheres, respectively. Taking into account the wire mean length (4 µm) and the diameter (1.7 nm) of the NWs and NSs, one can estimate a population of spheres approximatively 1200 times larger in number than the wire population in the mother liquor.

In the present work, a purification process was necessary to remove the excess of surfactants in order to make possible their directed assembly by nanoxerography (see experimental section for further details). This purification could modify the surface chemistry of the nanowires and nanospheres and their relative population. Therefore, SAXS measurements were performed on both as prepared and purified nanowires in liquid phase (Figure 2b). In both cases, self-assembly of the nanowires in solution was observed with time, as evidenced by the presence of Bragg peaks at very small angles. The peak positions in both cases characterized an hexagonal array of parallel nanowires.[29] The parameter of the hexagonal phases inferred from the peak positions was a = 9.7 ± 0.1 nm and a = 5.5 ± 0.1 nm respectively for the as-grown and purified nanowires. The lattice parameter corresponds to the center to center distance and is the sum of the wire diameter and the inter-wire spacing.[29] Taking into account that the wire diameter does not change with the purification process, as showed by TEM, one can conclude that the inter-wire distance in the self-assembled array decreased from 8 nm down to 3.8 nm after purification. This latter distance corresponds approximately to twice the oleylamine length, in agreement with a model of Au NWs surrounded by a single layer of surfactants. XPS performed on the purified Au NWs revealed the presence of Cl^- ions and nitrogen in both NH_2 (oleylamine) and NH_3^+ (oleylammonium) environment (Figure S1, supporting information). Thus, it appears that the

purified Au NWs used for the nanoxerography experiments were stabilized by a single layer of oleylamine / oleylammonium chloride.

3.2. Directed assembly of the gold colloids by AFM nanoxerography

Figure 3a presents a typical KFM image of two 3 µm charge squares of opposite polarities written by AFM on a 100 nm PMMA film. Using the charging conditions described in the experimental section, the surface potential of the upper (resp. bottom) square was + 6 V (resp. -6 V). After development in the purified colloidal suspension for 10 s, AFM observations revealed that gold NWs and NSs were selectively grafted onto charge patterns (Figures 3b-d). Gold NWs were exclusively assembled onto the positively charged square. The mean length of the assembled NWs was 4.2 ± 1.2 µm, proving that NWs were not altered during their selective assembly. This is remarkable as we reported that these NWs are extremely fragile and easily segmented under a high energy electron beam.[7] We demonstrate here that AFM nanoxerography can achieve such directed assembly without damaging Au NWs: electrostatic forces generated by charge patterns are sufficient to trap them onto the surface without breaking them. It is to be noted that this is the first time that colloidal nanowires with a length of a few micrometers are successfully assembled on surfaces by AFM nanoxerography. Figure 3d shows that gold nanospheres were assembled onto the negatively charged pattern with a high density. Nevertheless, a few NSs were also grafted on the positively charged pattern. This result shows that AFM nanoxerography allowed sorting efficiently the two kinds of nano-objects (NWs and NSs) present in the colloidal suspension.

Kinetic study of the colloid directed assembly

A study of the assembly kinetics was performed by varying the development time in the colloidal suspension. Similar charged squares as those presented in Figure 3a were written by AFM. AFM observations revealed that 2 NWs/µm² were trapped on the positive charge pattern (Figure 4a) while 56 NSs/µm² were trapped on the negative charge pattern (Figure 4d) after only a 5 s development. The density of NSs grafted on the positive charge pattern was very low and did not prevent any assembly of NWs. Similarly, the density of NWs grafted on the positive charge pattern left enough space to trap NSs. These results show that there was no competition between nanowires and nanospheres during the assembly process and that, as one could expected, the number of NWs and NSs grafted on each charge pattern strongly increase with the development time (Figures 4a-c and 4d-f). Densities of 6 NWs/µm² and 442 NSs/µm² were observed after a 30s development. It is to be noted that the mean length of the assembled NWs is 4.3 ± 2.5 µm, confirming that NWs were unharmed during the trapping process.

Determination of the** ion organization at the surface **of the gold colloids

Directed assembly of gold NWs and NSs on charge patterns of opposite polarities (Figures 3 and 4) gives direct information on the ion organization at the surface of these colloidal nano-objects. During the development step, two electrostatic forces generated by the local electric field created by charge patterns, act indeed on the NWs and NSs: the electrophoretic forces and the dielectrophoretic forces (Figure 5).[31] Electrophoretic forces describe the Coulomb interaction between charged nano-objects in suspension and the electric field generated by the charge patterns. They cause nano-objects carrying an effective charge to be attracted by oppositively charged patterns and repelled by like charge patterns. In addition, the presence of charge patterns

induces an electric field gradient which interacts with polarizable nano-objects. The distortion of their electrical double layer yields dipoles which interact with the non-uniform electric field and result in dielectrophoretic forces. The high polarizability of the gold nano-objects in hexane leads to attractive dielectrophoretic forces, independent of the charge polarity of the patterns.[32] On this basis, experimental results presented in Figures 3 and 4 clearly suggest that gold NWs present a negative effective charge close to the charge patterns. As depicted on figure 5, the NWs thus assembled on the positive charge pattern through both attractive electrophoretic and dielectrophoretic forces. No nanowire was assembled on the negative charge pattern because attractive dielectrophoretic forces were not sufficient to counterbalance the strong repulsive electrophoretic forces on the negative charge pattern. In the case of NSs, the difference of density observed on the patterns, high (resp. weak) density on the negative (resp. positive) pattern, indicates that the gold NSs present only a small positive effective charge, leading to a balance between dielectrophoretic and electrophoretic forces (Figure 5). On the positive charge pattern, repulsive electrophoretic forces were insufficient to fully compensate the attractive dielectrophoretic forces resulting into a weak density of grafted nanospheres. On the contrary, a high density of NSs was trapped onto the negative charge pattern where both electrophoretic and dielectrophoretic forces were attractive.

Following the Derjaguin–Landau–Verwey–Overbeek (DLVO) theory, the charge separation between the ions adsorbed at the surface of the colloids and the diffuse counter ions layer is favoured by a large dielectric constant of the solvent and by a low ionic strength. On the contrary, apolar solvent, like hexane, are well known to favour the formation of ion pairs because of their very small dielectric constant. Therefore, colloidal suspension in hexane should be

strongly unfavourable for electrophoretic forces. Dielectrophoretic forces were thus expected to be the predominant driving forces for assembly in our case.

Actually, examples of nanoparticle self-assemblies driven by electrophoretic interactions from colloidal suspensions in an apolar solvent are scarce. Shevshenko *et al.* showed that metal and metal oxide nanoparticles in toluene could exhibit an electrophoretic mobility with a sign that depends on the nature of the organic ligand at their surface.[33] Binary assemblies presenting a structure analogous to that of ionic crystals were obtained by mixing oppositely charged nanoparticles in a mixture toluene-chloroform. Martin *et al.* described the synthesis in water of charged nanoparticles and their transfer into hexane with dodecanethiol as coating agent.[34] The resulting particles in hexane exhibited a negative charge, which played an important role for the particle self-assembly at the interface air-toluene.

In our case, it is unlikely that the NWs and NSs in suspension in hexane exhibit a net charge because of the very low polarity of the solvent. The effective charge revealed by the nanoxerography experiments may result from the presence of the strong electrical field generated by the charge patterns. For the wires in hexane, the chloride anions associated to oleylammonium cations insure their global charge neutrality and their steric stabilization as showed by XPS analysis. The effective negative charge of the gold nanowires evidenced by nanoxerography (Figures 3 and 4) suggests that the chloride ions are linked to the gold surface atoms and that during the development in the colloidal suspension, the strong electric field generated by the positively charged pattern probably separates the {gold + chloride ions} core from the ammonium layer as illustrated on Figure 6a. A direct measurement of the electrophoretic mobility of the NWs would confirm this assumption, but unfortunately our attempts have not been successful so far, probably because of the non-spherical shape of the objects. More amazing

is the very different behaviour of the small NSs which were present in solution together with the NWs and exhibited a small positive charge revealed by a preferential assembly on the negative pattern. An effective positive charge on gold nanospheres coated with bromide ions and quaternary ammoniums was already evidenced by AFM nanoxerography.[26] In the present case, this positive charge is probably due to a second shell of oleylammonium cations interdigitated with the first shell through strong Van der Waals interaction (Figure 6b). A bilayer of long chain ammonium around NSs has already been described in the case of ZnO particles.[35] Such a bilayer could explain a difference in the electrophoretic mobility of the NSs and NWs. It suggests that the spherical geometry is more favourable for the ammonium interdigitation.

3.3. Directed assembly of single gold nanowires

On the basis of these results, directed assembly of single gold NWs by AFM nanoxerography was studied. Figure 7a displays KFM images of four patterned lines of charged dots using different voltage pulse amplitudes and spacings between each dot. From the left to the right, the surface potential, the spacing between each dot and the width of the resulting lines of charged dots were +1.2 V / 400 nm / 470 nm, +1.4 V / 200 nm / 460 nm, +1.26 V / 200 nm / 314 nm and +0.25 V / 50 nm / 205 nm respectively. Except for the left pattern, all the patterned dots appear as continuous charged lines due to a lack of lateral resolution in KFM and diffusion of charges within the PMMA film.[36] After development in the colloidal suspension, Figure 7b reveals that for charged dots of +1.2 V / 470 nm, coiling of NWs occurred on each dot, without any NW interconnections of adjacent dots. Bending radii as small as 40 nm were measured on the NWs without any visible breaking, evidencing the remarkable flexibility of these 1D gold nanowires. Below 200 nm spacing between dots, NWs were connected to each dot of the charge pattern, resulting into nice alignment of the gold NWs along the charged lines. 5 NWs were assembled

along the 460 nm wide charged line presenting a +1.4 V surface potential, while only 2 NWs were assembled along the 314 nm charged line with a +1.26 V surface potential, showing that the number of grafted NWs can be controlled by a fine tuning of the surface potential and the width of the dotted line. A single NW was perfectly aligned along the charge line in the case +0.25 V / 50 nm / 205 nm charged line. Such assemblies of gold NW open the way to further investigation of their mechanical and conductive properties.

4. Conclusion

Directed assembly of colloidal gold nanowires and nanospheres, from their hexane solution onto specific areas of surfaces, has been achieved by AFM nanoxerography in a few seconds. Despite the very low polarity of hexane that makes this solvent strongly unfavorable for charge separation, a selective assembly of the NWs only occurred onto positive charge patterns written by AFM while the NSs essentially assembled on negative charge patterns. These results suggest the appearance of an effective charge on the nano-objects due to the very strong electric field in solution at the vicinity of the charge patterns. The negative effective charge of the nanowires was interpreted by a first shell of chloride ions strongly bonded to the wire surface and a second shell of mobile ammonium cations. The positive effective charge of the spheres was interpreted as resulting from a second layer of oleylammonium cations interdigitated through strong Van der Waals interactions.

AFM nanoxerography is therefore an efficient way to give information on the ion organization at the surface of colloids, and, in the present case, to sort colloidal suspension composed of two kinds of nano-objects. This study finally reveals the capabilities of AFM nanoxerography to

assemble single gold NWs with very high aspect ratio (1:2100) onto pre-defined areas of surfaces without damaging them, opening the way to further investigations of the properties of single NWs or other highly anisotropic nano-objects such as carbon nanotubes or DNA strands.

FIGURES

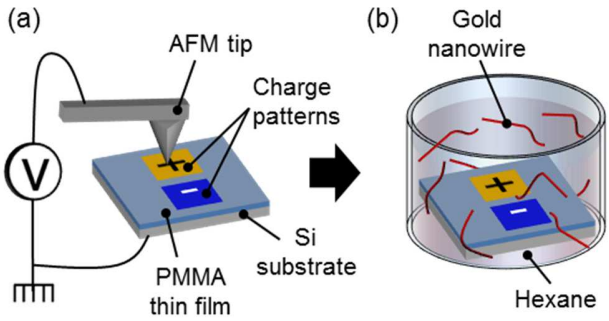

Figure 1. Directed assembly of gold nanowires by AFM nanoxerography: (a) AFM charge writing, (b) development by immersion in the gold colloidal suspension

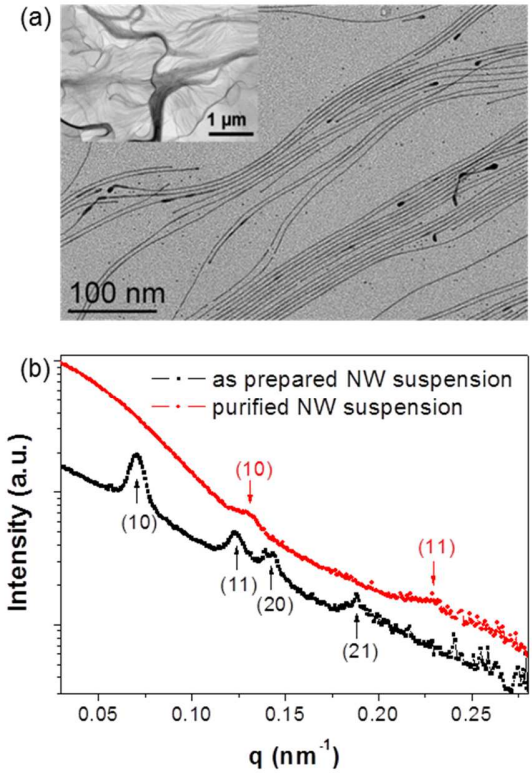

Figure 2. (a) TEM image of the purified colloidal suspension exhibiting gold nanowires and nanospheres. The low magnification TEM image in the inset shows the micrometric length of the nanowires, (b) SAXS data of the hexagonal phase of as-grown (black) and purified (red) gold nanowires. The peak positions in the reciprocal space relative to the position of the first peak are 1:√3:√4:√7 for the as-grown and 1:√3 for the purified nanowires.

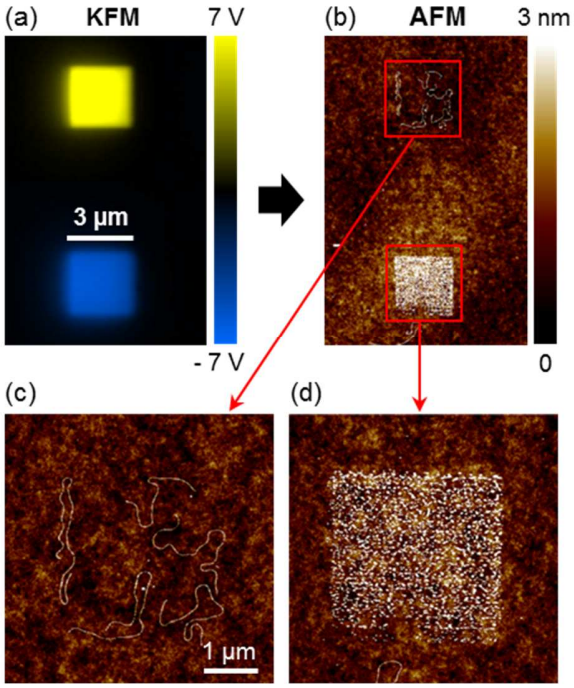

Figure 3. Directed assembly of gold nanowire suspension by AFM nanoxerography on 3 µm charge squares of opposite polarities: (a) KFM image of two 3 µm charge squares of opposite polarities written by AFM on a 100 nm PMMA film, (b) to (d) AFM topographical images of the resulting assembly of gold nanowires and nanospheres on charge squares presented in (a) after development in the gold NW colloidal suspension for 10 s.

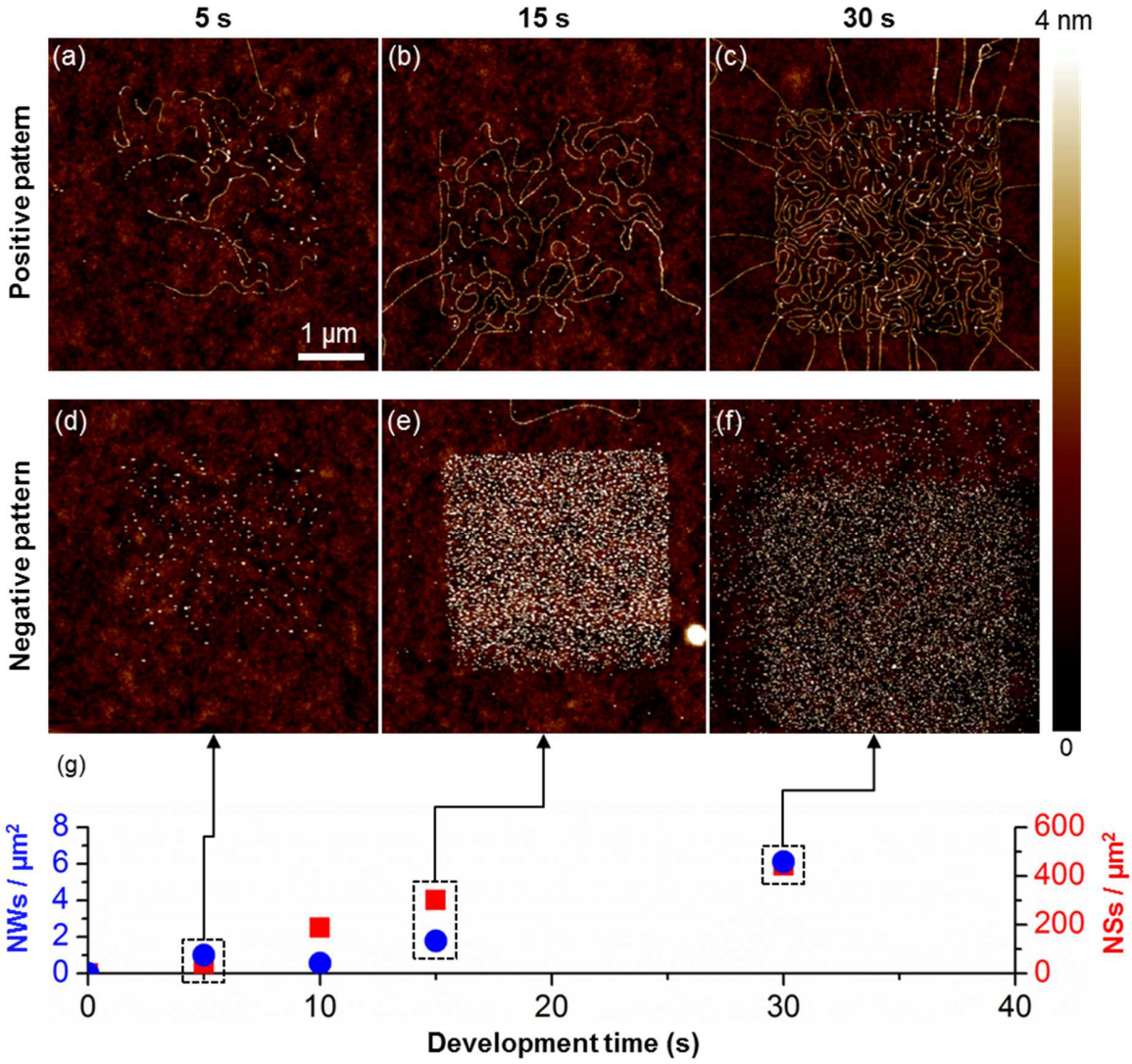

Figure 4. AFM images of positive (a-c) and negative (d-f) charge squares after 5, 15 and 30 s of development into the colloidal gold NW suspension, and (g) evolution as a function of the development time of the NW and NS density on positive and negative charge patterns respectively.

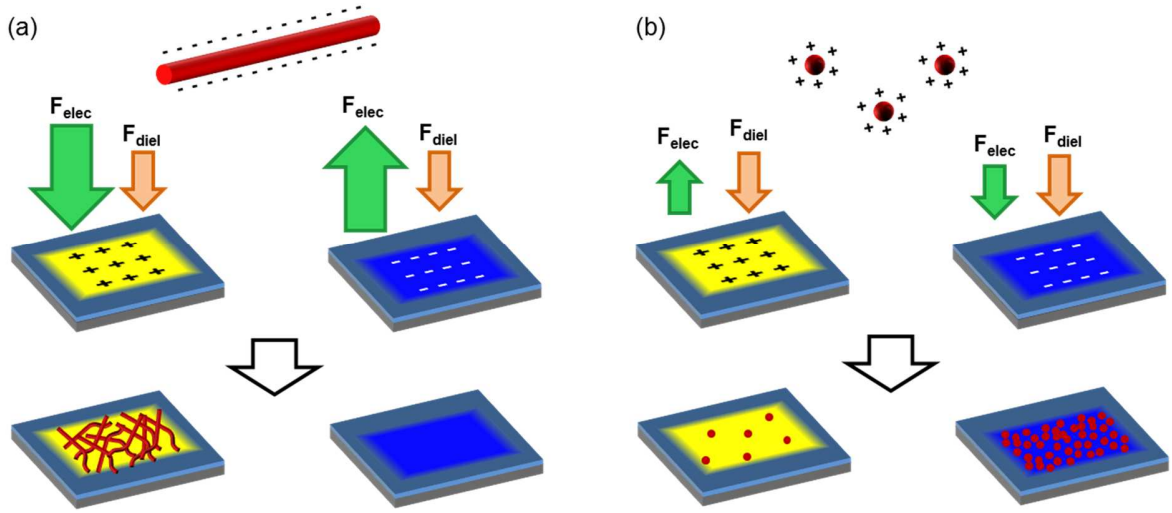

Figure 5. Schematics of the electrophoretic (F_{elec}) and dielectrophoretic (F_{diel}) forces exerted by charge patterns of opposite polarities on the gold (a) nanowires and (b) nanospheres. The size of the coloured arrows indicates the amplitude of the electrostatic forces.

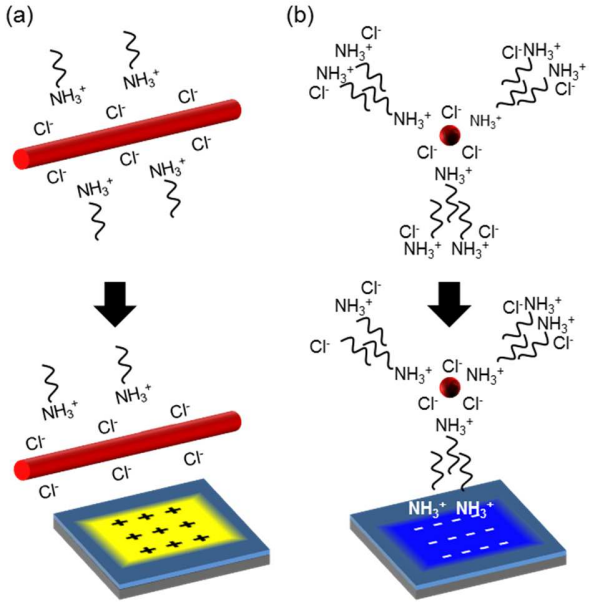

Figure 6. Schematics of the surface stabilisation of gold (a) nanowires and (b) nanospheres, far from the charge patterns and near them. The repartitions of chloride anions and oleylammonium are drastically modified by the presence of charge patterns, resulting in effective charges.

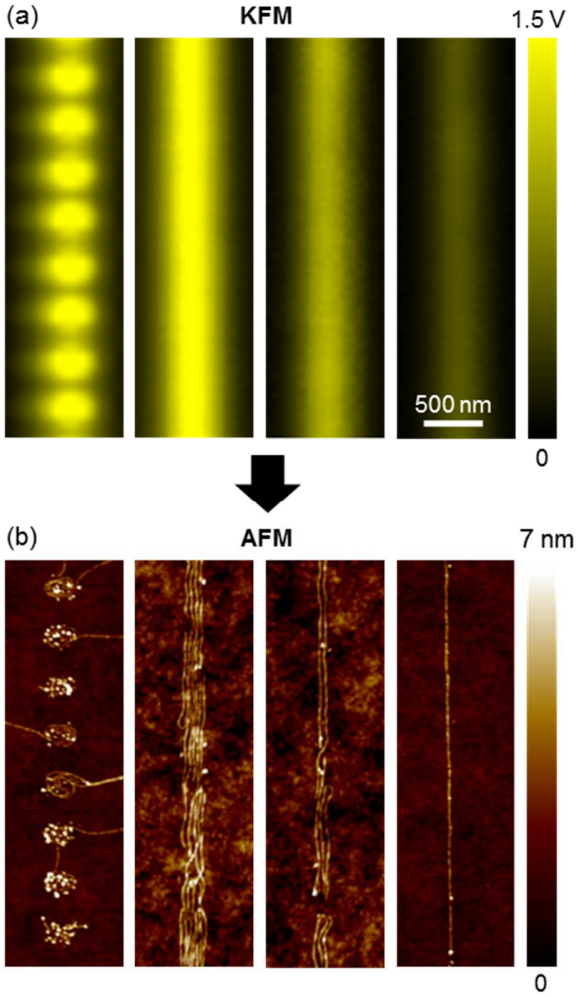

Figure 7. (a) KFM images of four charged dotted lines written by AFM using different voltage pulse amplitudes and spacing between dots: from the left to the right, the amplitude of the voltage pulses and the spacing between each dot were +75 V / 400 nm, +70 V / 200 nm, + 55 V / 200 nm and + 30 V / 50 nm; (b) AFM topographical image of the directed assembly of gold NWs on the dotted lines presented in (a) by AFM nanoxerography.

ASSOCIATED CONTENT

Supporting Information. XPS spectra of purified Au nanowires are available free of charge via the Internet at http://pubs.acs.org.

AUTHOR INFORMATION

Corresponding Author

* Dr Lise-Marie Lacroix. lmlacroi@insa-toulouse.fr. Tel : +33567048833 .Fax : +33561559697

* Pr Laurence Ressier. laurence.ressier@insa-toulouse.fr. Tel : +33561559657 .Fax : +33561559697

Author Contributions

The manuscript was written through contributions of all authors.

ACKNOWLEDGMENT

Romuald Poteau (LPCNO, Toulouse) is warmly thanked for fruitful discussions. The authors also thank G. Antorrena (INA, Saragossa) for XPS measurements. They finally acknowledge the financial support of the Labex NEXT, N° 11 LABX 075.

REFERENCES

(1) Chen, J.; Wiley, B. J.; Xia, Y. One-Dimensional Nanostructures of Metals: Large-Scale Synthesis and Some Potential Applications. *Langmuir* **2007**, *23*, 4120–4129.

(2) Wetz, F.; Soulantica, K.; Respaud, M.; Falqui, A.; Chaudret, B. Synthesis and Magnetic Properties of Co Nanorod Superlattices. *Mater. Sci. Eng. C* **2007**, *27*, 1162–1166.

(3) Feng, H.; Yang, Y.; You, Y.; Li, G.; Guo, J.; Yu, T.; Shen, Z.; Wu, T.; Xing, B. Simple and Rapid Synthesis of Ultrathin Gold Nanowires, Their Self-Assembly and Application in Surface-Enhanced Raman Scattering. *Chem. Commun.* **2009**, 1984.

(4) Chandni, U.; Kundu, P.; Singh, A. K.; Ravishankar, N.; Ghosh, A. Insulating State and Breakdown of Fermi Liquid Description in Molecular-Scale Single-Crystalline Wires of Gold. *ACS Nano* **2011**, *5*, 8398–8403.

(5) Roy, A.; Pandey, T.; Ravishankar, N.; Singh, A. K. Single Crystalline Ultrathin Gold Nanowires: Promising Nanoscale Interconnects. *AIP Adv.* **2013**, *3*, 032131.

(6) Pud, S.; Kisner, A.; Heggen, M.; Belaineh, D.; Temirov, R.; Simon, U.; Offenhäusser, A.; Mourzina, Y.; Vitusevich, S. Features of Transport in Ultrathin Gold Nanowire Structures. *Small* **2013**, *9*, 846–852.

(7) Lacroix, L.-M.; Arenal, R.; Viau, G. Dynamic HAADF-STEM Observation of a Single-Atom Chain as the Transient State of Gold Ultrathin Nanowire Breakdown. *J. Am. Chem. Soc.* **2014**. *136*, 13075-13077

(8) Wang, C.; Hu, Y.; Lieber, C. M.; Sun, S. Ultrathin Au Nanowires and Their Transport Properties. *J. Am. Chem. Soc.* **2008**, *130*, 8902–8903.

(9) Sánchez-Iglesias, A.; Rivas-Murias, B.; Grzelczak, M.; Pérez-Juste, J.; Liz-Marzán, L. M.; Rivadulla, F.; Correa-Duarte, M. A. Highly Transparent and Conductive Films of Densely Aligned Ultrathin Au Nanowire Monolayers. *Nano Lett.* **2012**, *12*, 6066–6070.

(10) Chen, Y.; Ouyang, Z.; Gu, M.; Cheng, W. Mechanically Strong, Optically Transparent, Giant Metal Superlattice Nanomembranes From Ultrathin Gold Nanowires. *Adv. Mater.* **2013**, *25*, 80–85.

(11) Kisner, A.; Heggen, M.; Mayer, D.; Simon, U.; Offenhäusser, A.; Mourzina, Y. Probing the Effect of Surface Chemistry on the Electrical Properties of Ultrathin Gold Nanowire Sensors. *Nanoscale* **2014**, *6*, 5146.

(12) Oshima, Y.; Mouri, K.; Hirayama, H.; Takayanagi, K. Quantized Electrical Conductance of Gold Helical Multishell Nanowires. *J. Phys. Soc. Jpn.* **2006**, *75*, 053705.

(13) Agraït, N.; Yeyati, A. L.; van Ruitenbeek, J. M. Quantum Properties of Atomic-Sized Conductors. *Phys. Rep.* **2003**, *377*, 81–279.

(14) Yoshihira, M.; Moriyama, S.; Guerin, H.; Ochi, Y.; Kura, H.; Ogawa, T.; Sato, T.; Maki, H. Single Electron Transistors with Ultra-Thin Au Nanowires as a Single Coulomb Island. *Appl. Phys. Lett.* **2013**, *102*, 203117.

(15) Guerin, H.; Yoshihira, M.; Kura, H.; Ogawa, T.; Sato, T.; Maki, H. Coulomb Blockade in a Granular Material Made of Gold Nanowires. In *2012 12th IEEE Conference on Nanotechnology (IEEE-NANO)*; 2012; pp 1–5.

(16) Loubat, A.; Escoffier, W.; Lacroix, L.-M.; Viau, G.; Tan, R.; Carrey, J.; Warot-Fonrose, B.; Raquet, B. Cotunneling Transport in Ultra-Narrow Gold Nanowire Bundles. *Nano Res.* **2013**, *6*, 644–651.

(17) Demers, L. M.; Mirkin, C. A. Combinatorial Templates Generated by Dip-Pen Nanolithography for the Formation of Two-Dimensional Particle Arrays. *Angew. Chem. Int. Ed.* **2001**, *40*, 3069–3071.
(18) Malaquin, L.; Kraus, T.; Schmid, H.; Delamarche, E.; Wolf, H. Controlled Particle Placement through Convective and Capillary Assembly. *Langmuir* **2007**, *23*, 11513–11521.
(19) Khondaker, S. I.; Luo, K.; Yao, Z. The Fabrication of Single-Electron Transistors Using Dielectrophoretic Trapping of Individual Gold Nanoparticles. *Nanotechnology* **2010**, *21*, 095204.
(20) Junno, T.; Deppert, K.; Montelius, L.; Samuelson, L. Controlled Manipulation of Nanoparticles with an Atomic Force Microscope. *Appl. Phys. Lett.* **1995**, *66*, 3627–3629.
(21) Mesquida, P.; Stemmer, A. Attaching Silica Nanoparticles from Suspension onto Surface Charge Patterns Generated by a Conductive Atomic Force Microscope Tip. *Adv. Mater.* **2001**, *13*, 1395–1398.
(22) Mesquida, P.; Stemmer, A. Maskless Nanofabrication Using the Electrostatic Attachment of Gold Particles to Electrically Patterned Surfaces. *Microelectron. Eng.* **2002**, *61–62*, 671–674.
(23) Tzeng, S.-D.; Lin, K.-J.; Hu, J.-C.; Chen, L.-J.; Gwo, S. Templated Self-Assembly of Colloidal Nanoparticles Controlled by Electrostatic Nanopatterning on a Si3N4/SiO2/Si Electret. *Adv. Mater.* **2006**, *18*, 1147–1151.
(24) Barry, C. R.; Steward, M. G.; Lwin, N. Z.; Jacobs, H. O. Printing Nanoparticles from the Liquid and Gas Phases Using Nanoxerography. *Nanotechnology* **2003**, *14*, 1057.
(25) Palleau, E.; Sangeetha, N. M.; Viau, G.; Marty, J.-D.; Ressier, L. Coulomb Force Directed Single and Binary Assembly of Nanoparticles from Aqueous Dispersions by AFM Nanoxerography. *ACS Nano* **2011**, *5*, 4228–4235.
(26) Ressier, L.; Palleau, E.; Garcia, C.; Viau, G.; Viallet, B. How to Control AFM Nanoxerography for the Templated Monolayered Assembly of 2 Nm Colloidal Gold Nanoparticles. *IEEE Trans. Nanotechnol.* **2009**, *8*, 487–491.
(27) Sangeetha, N. M.; Moutet, P.; Lagarde, D.; Sallen, G.; Urbaszek, B.; Marie, X.; Viau, G.; Ressier, L. 3D Assembly of Upconverting NaYF4 Nanocrystals by AFM Nanoxerography: Creation of Anti-Counterfeiting Microtags. *Nanoscale* **2013**, *5*, 9587–9592.
(28) Seemann, L.; Stemmer, A.; Naujoks, N. Selective Deposition of Functionalized Nano-Objects by Nanoxerography. *Microelectron. Eng.* **2007**, *84*, 1423–1426.
(29) Loubat, A.; Impéror-Clerc, M.; Pansu, B.; Meneau, F.; Raquet, B.; Viau, G.; Lacroix, L.-M. Growth and Self-Assembly of Ultrathin Au Nanowires into Expanded Hexagonal Superlattice Studied by in Situ SAXS. *Langmuir* **2014**, *30*, 4005–4012.
(30) Ressier, L.; Nader, V. L. Electrostatic Nanopatterning of PMMA by AFM Charge Writing for Directed Nano-Assembly. *Nanotechnology* **2008**, *19*, 135301.
(31) Palleau, E.; Sangeetha, N. M.; Ressier, L. Quantification of the Electrostatic Forces Involved in the Directed Assembly of Colloidal Nanoparticles by AFM Nanoxerography. *Nanotechnology* **2011**, *22*, 325603.
(32) Pohl, H. A. *Dielectrophoresis: The Behavior of Neutral Matter in Nonuniform Electric Fields*; Cambridge monographs on physics; Cambridge University Press: Cambridge ; New York, 1978.

(33) Shevchenko, E. V.; Talapin, D. V.; Kotov, N. A.; O'Brien, S.; Murray, C. B. Structural Diversity in Binary Nanoparticle Superlattices. *Nature* **2006**, *439*, 55–59.
(34) Martin, M. N.; Basham, J. I.; Chando, P.; Eah, S.-K. Charged Gold Nanoparticles in Non-Polar Solvents: 10-Min Synthesis and 2D Self-Assembly. *Langmuir* **2010**, *26*, 7410–7417.
(35) Pagès, C.; Coppel, Y.; Kahn, M. L.; Maisonnat, A.; Chaudret, B. Self-Assembly of ZnO Nanocrystals in Colloidal Solutions. *ChemPhysChem* **2009**, *10*, 2334–2344.
(36) Jacobs, H. O.; Leuchtmann, P.; Homan, O. J.; Stemmer, A. Resolution and Contrast in Kelvin Probe Force Microscopy. *J. Appl. Phys.* **1998**, *84*, 1168–1173.

Insert Table of Contents Graphic and Synopsis Here